

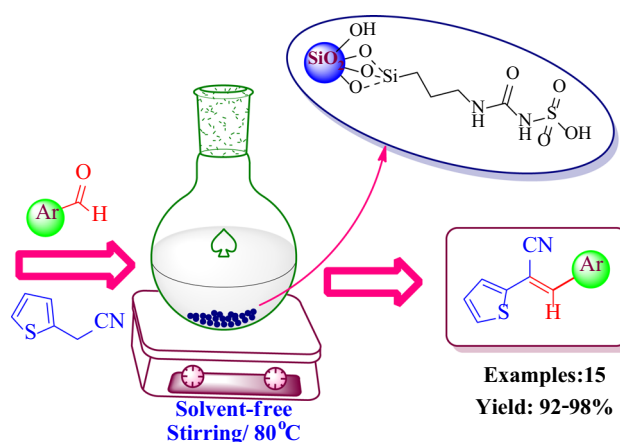
Silica Bonded *N*-(Propylcarbamoyl)sulfamic acid (SBPCSA) Mediated Expeditious Approach to C–C Bond Formation: An Innovative Pathway for Acrylonitrile Derivatives

Mehtab Parveen¹ · Shaista Azaz¹ · Faheem Ahmad¹ · Ali Mohammed Malla¹ · Mahboob Alam²

Received: 18 April 2016 / Accepted: 11 June 2016
© Springer Science+Business Media New York 2016

Abstract A new silica bonded *N*-(propylcarbamoyl)sulfamic acid (SBPCSA) catalyst has been prepared for the highly efficient synthesis of a series of acrylonitrile derivatives via solvent-free facile Knoevenagel condensation between differently substituted heterocyclic/aromatic aldehydes **1** (a–o) and 2-thiopheneacetonitrile (**2**). The catalyst was characterized by FT-IR, SEM-EDX and XRD techniques. The thermal stability of the catalyst was evaluated with TGA and DT analysis. The remarkable features of the present protocol are solvent free synthesis, recyclability of the catalyst, mild reaction conditions, shorter reaction profile, excellent yield of products with applicability to broader substrate scope (electron rich and electron deficient) and exclusive formation of *E*-isomer of the product. DFT calculations also revealed that *E*-isomer of compound **3f** is stabilized by 12.53 kcal mol⁻¹ more than the *Z*-isomer.

Graphical Abstract Efficient and economical synthesis of acrylonitrile derivatives.



Keywords Acrylonitrile · SBPCSA · Knoevenagel condensation · *E*-isomer · DFT studies

1 Introduction

In the last few decades, there has been an upsurge usage for environmentally benign and sustainable catalyst in the chemical industry [1, 2]. Recycling of homogeneous catalysts is the main issue in large-scale production of chemicals [3]. In this regard, substantial research efforts have been devoted to develop catalysts with high efficacy, selectivity and stability. Immobilization of catalysts on solid support, leads to clean chemical synthesis for environmental as well as economical point of view [4, 5]. Heterogeneous catalysts have gained much attraction of

Electronic supplementary material The online version of this article (doi:10.1007/s10562-016-1793-7) contains supplementary material, which is available to authorized users.

✉ Mehtab Parveen
mehtab.organic2009@gmail.com

¹ Division of Organic Synthesis, Aligarh Muslim University, Aligarh 202002, India

² Division of Bioscience, Dongguk University, Gyeongju 780-714, Republic of Korea

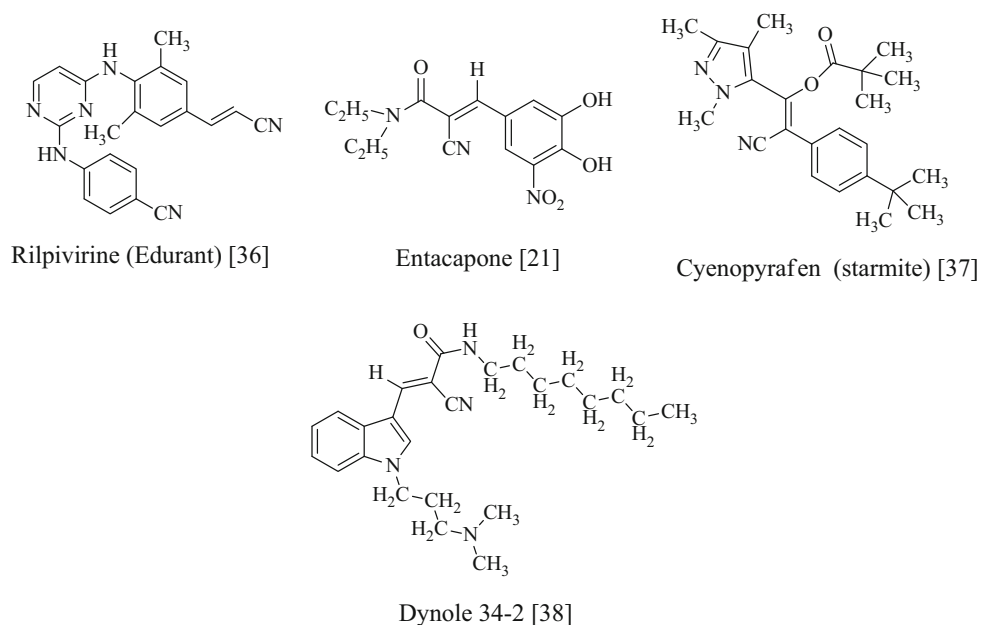


Fig. 1 Drugs in the market with acrylonitrile moiety in their structural framework

chemist due to economic and environmental importance [6]. These catalysts are advantageous over homogeneous catalysts as they can be easily recovered from the reaction mixture by simple filtration and can be reused after activation, thereby making the process economically valuable. Due to the favorable chemical and physical properties of silica surfaces, it is possible to impart any reactive functional group e.g., sulfonic, amine, carboxyl and thiol etc. on silica surfaces through well-known silane chemistry [7, 8]. Therefore, use of supported and recoverable catalysts in organic transformations has economical and environmental benefits [9]. In this regards, carbon based solid acid catalysts have attracted much more attention due to more activity and selectivity [10–12]. These sulfonated silica/carbon hybrids have been prepared from the sulfonation of carbonized biomaterials have been extensively used in organic syntheses [13–15].

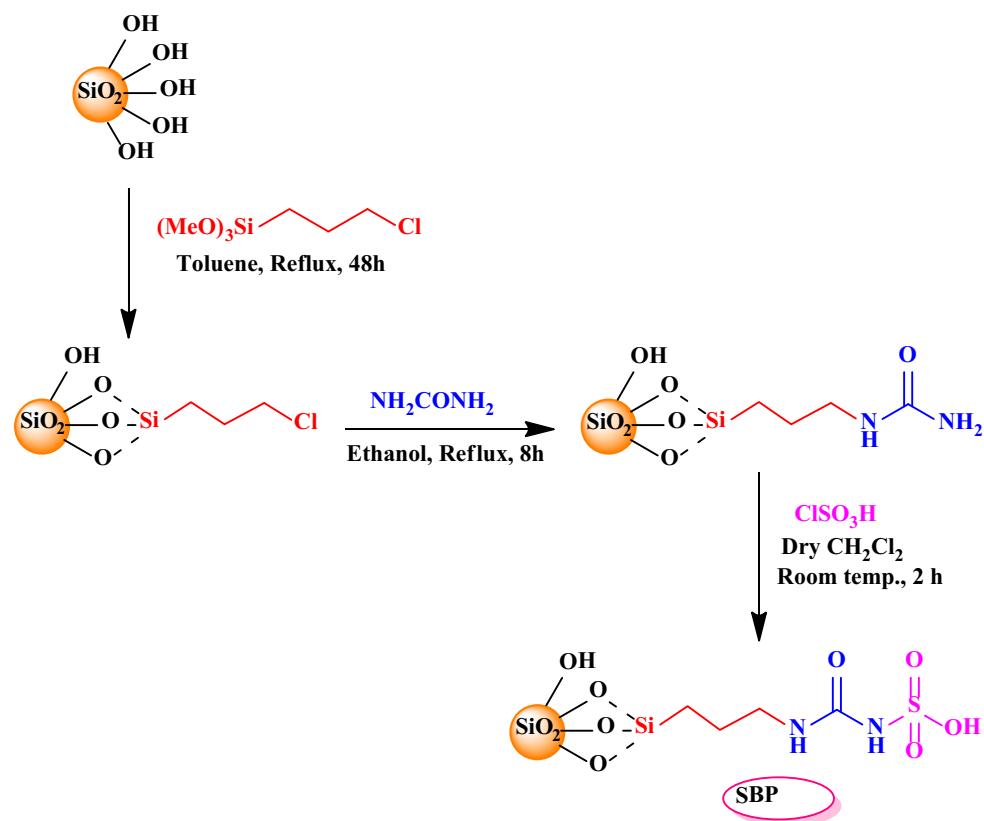
Carbon–carbon (C–C) bond formation reactions are of significant importance in organic synthesis as they unlock new pathways to new chemical entities [16–18]. The Knoevenagel condensation between aldehydes and ketones with activated methylene compounds is one of the reactions which facilitates C–C bond formation [19, 20] and has been exploited in the synthesis of some vital drugs such as entacapone [21] pioglitazone [22] and lumefantrine [23]. The use of ammonia, amines, pyridine, piperidine and their salts as basic catalysts in Knoevenagel condensation restricts their applications due to their hazardous environmental concerns, carcinogenic nature, problem in product

separation and reusability [24]. Therefore there is a need for exploring the cheap and easily available catalysts for Knoevenagel condensation.

Over the past few decades there has been an upsurge in the number of biologically active compounds that contain an acrylonitrile moiety. Acrylonitrile derivatives constitute an important class of compounds in organic chemistry due to their promising biological activities such as antiproliferative [25], antifungal [26], antitumor [27], antibacterial [28], antitubercular [29], antioxidative [30, 31], tuberculostatic [32], antitrichomonal [33] and antiparasitic [34]. Various medicinally important drugs also possess acrylonitrile moiety in their structural framework viz. DG172 [35], Rilpivirine (Edurant) [36] Entacapone [21], Cyenopyrafen [37] and Dynole 34-2 [38] (Fig. 1).

The synthesis of acrylonitrile compounds have been previously achieved by the use of Wittig reactions [39], McMurry coupling [40] and the Heck reaction [41]. It is pertinent to mention here that Knoevenagel condensation is a facile and versatile method for the formation of acrylonitrile derivatives [42–44]. In the quest to achieve higher efficiency several catalysts have been employed viz Brønsted acid catalysts [45], Lewis acids such as $\text{MgBr}_2 \cdot \text{OEt}_2$ [46], SnCl_2 [47], Al_2O_3 [48] ionic liquids $[\text{C}_6\text{-mim}]\text{PF}_6$ [49], $[\text{Bmim}]\text{Cl} \cdot x\text{AlCl}_3$ [50], $[\text{Bpy}]\text{Cl} \cdot x\text{AlCl}_3$ [50], $[\text{Bmim}]\text{BF}_4$ [51], ethylammonium nitrate (EAN) [52] and silica supported acid catalyst [53, 54].

In continuation of our ongoing interest for exploring novel synthetic methodologies for organic transformations



Scheme 1 Synthetic scheme for the formation of catalyst SBPCSA

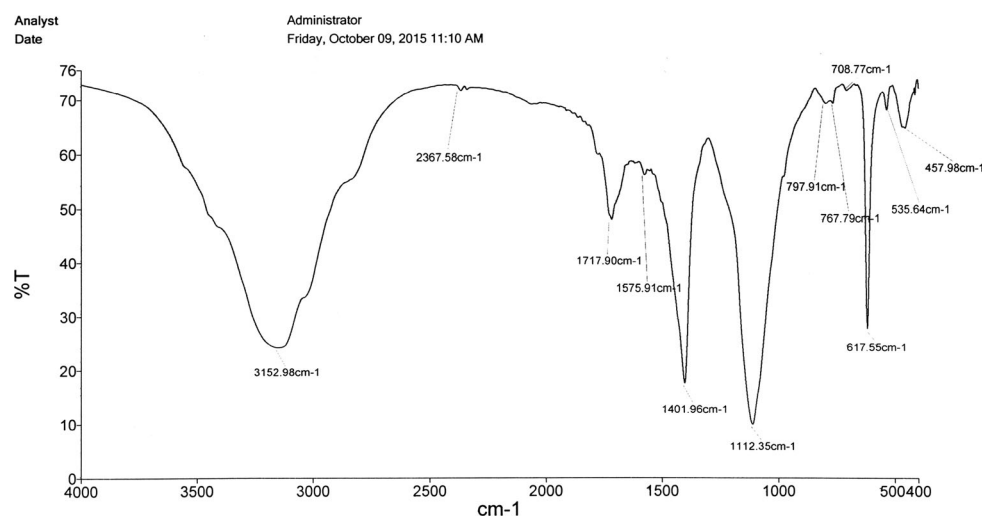


Fig. 2 FT-IR spectrum of the catalyst SBPCSA

[55, 56] under the principle of green chemistry, herein, we first time report the synthesis of novel silica bonded *N*-(propylcarbamoyl)sulfamic acid (SBPCSA) as a green, efficient and recyclable catalyst for the synthesis of

acrylonitrile derivatives. In comparison with the present reported methods of acrylonitrile synthesis, our approach displays specific advantages and become more practical than existing synthetic methodologies as it gives excellent

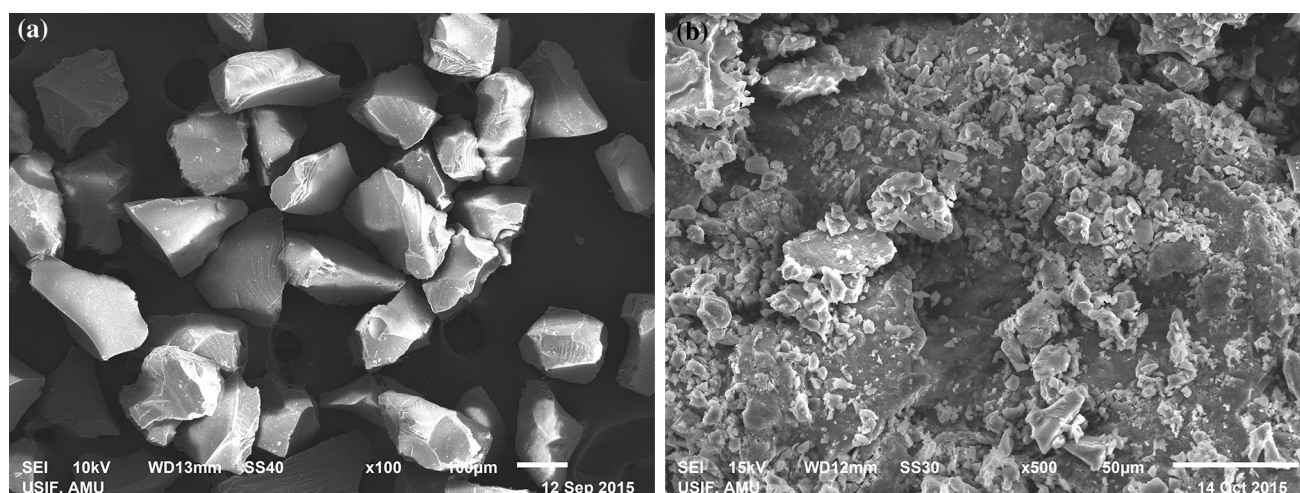


Fig. 3 SEM analysis of **a** SiO₂ **b** catalyst SBPCSA

yields (92–98 %) within a minimum reaction time and applicable to a broader substrate scope (electron-rich and electron-deficient).

2 Results and Discussion

2.1 Characterization of the Catalyst

The catalyst SBPCSA was prepared by the concise route outlined in Scheme 1. The SBPCSA was fully characterized by FT-IR, SEM-EDX and XRD. The FT-IR spectrum of the catalyst (SBPCSA) is depicted in Fig. 2. The FT-IR spectrum displayed peaks at 3152 cm⁻¹ attributed to the presence of the N–H bond stretching frequency of sulphonamide groups, which has been overlapped with O–H stretching frequency of silanol group or the adsorbed water molecules [57]. The corresponding C=O stretching and bending frequency of N–H were observed at 1717 and 1575 cm⁻¹, respectively. The peak at 1401.96 cm⁻¹ is assigned for C–H bending. Further, the peak at about 797 and 1112 cm⁻¹ is attributed to the typical symmetric stretching vibration of Si–O–Si and S=O bond of supported SO₃H group, respectively. Moreover stretching vibration of S–N bond in the –HN–SO₃H is observed at 767 cm⁻¹ [58].

To study the surface morphology of the catalyst, SEM micrographs of the catalyst was employed (Fig. 3). The SEM result showed the adsorption of *N*-(propylcarbonyl)sulfamic acid on silica surfaces. The composite is a fine homogeneous powder in which particles were of uneven size and shape, well dispersed on the surface of the silica gel. The successful incorporation of urea and SO₃H groups was also confirmed by EDX analysis (Fig. 4) of the catalyst, which showed the presence of N, S, O and Si

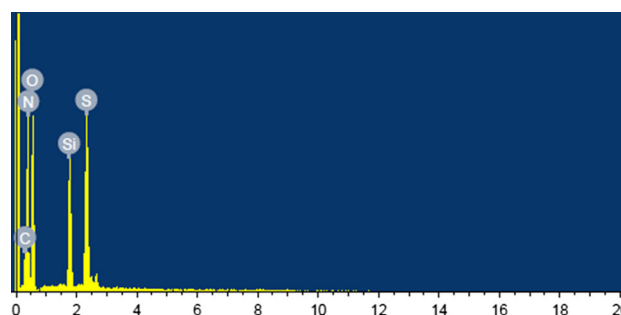


Fig. 4 EDX analysis of catalyst SBPCSA

elements signifying the formation of expected catalytic system. The weight % and atomic % of elements present in the catalyst has been showed in Table S1 (ESI). In the fresh catalyst S is present by weight % 13.38 and atomic % 6.79 while N is present by weight % 22.37 and atomic % 26.00. Further elemental mapping of the catalyst showed the uniform distribution of elements present in the catalyst (Fig. 5).

The chemical modification of silica support with *N*-(propylcarbonyl)sulfamic acid, was further explored by powder XRD analysis (Fig. 6). The XRD pattern of the catalyst were recorded in the 2θ range of 10°–80°. The XRD of the catalyst showed characteristic single broad peak of silica in the range of $2\theta = 18^\circ\text{--}25^\circ$ displaying amorphous nature of silica. However, the XRD of SBPCSA also showed crystallinity with the characteristic peaks of urea [59].

The thermal stability of the catalyst was evaluated by TG analysis (Fig. 7). The TG curve showed first weight loss of 62.84 % around 336 °C which can be attributed to the decomposition of amide chain along with SO₃H group

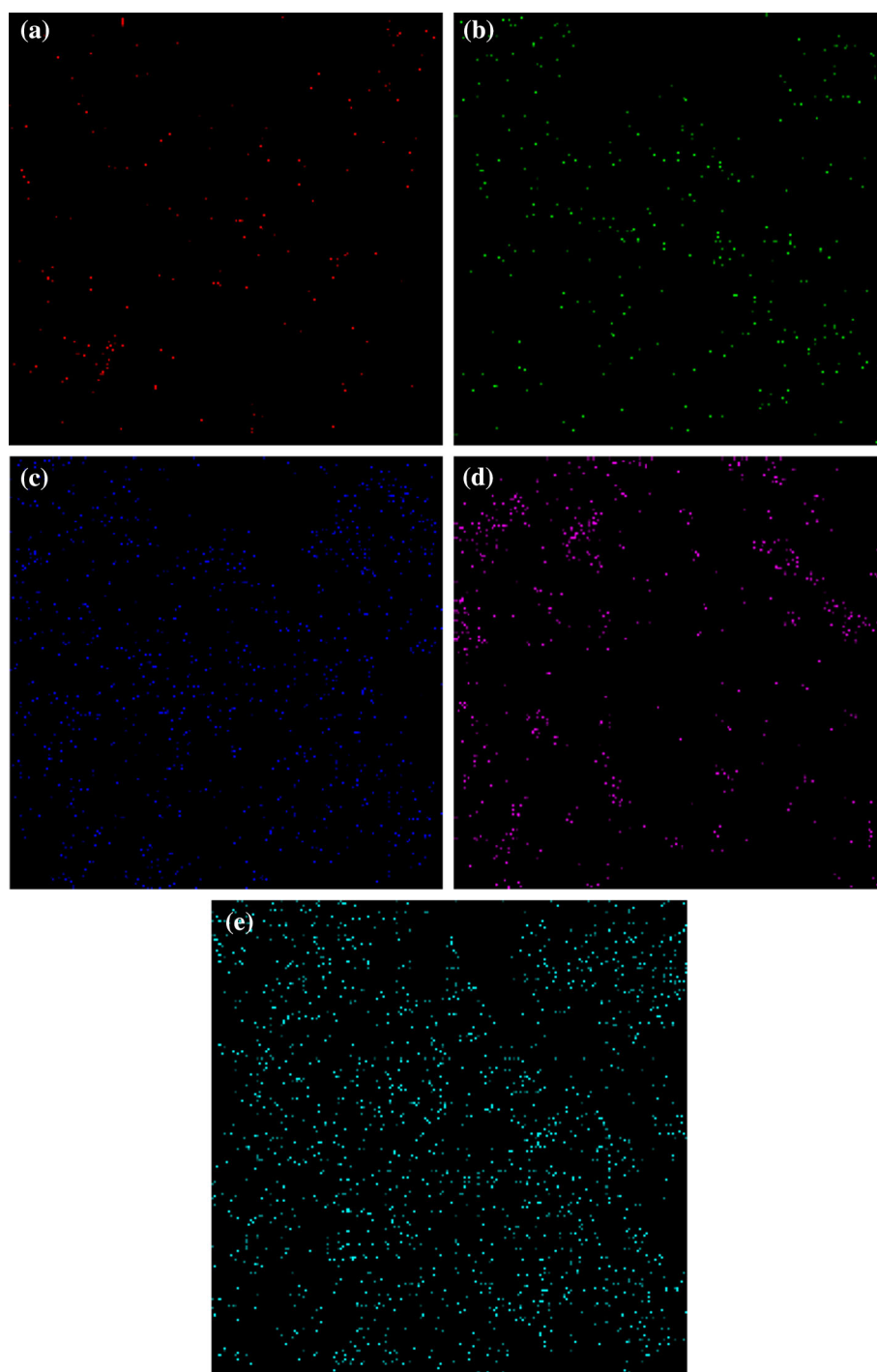


Fig. 5 Elemental mapping of catalyst SBPCSA **a** carbon **b** nitrogen **c** oxygen **d** silicon **e** sulfur showing uniform distribution of catalyst surface

and physically adsorbed water molecules. Further another weight loss of 9.1 % at 442 °C can be attributed to the loss of Si group covalently bonded to silica surface. Hence it can be concluded that catalyst is stable up to 336 °C. TGA is further supported by DT analysis (Fig. 7) in which a prominent peak at 297 and 365 °C showed endothermic

reaction which help in the removal of water, SO₃H group, amide moiety, Si group.

The optimum concentration of H⁺ ion was determined by acid–base titration of the aqueous suspension of the weighed amount of thoroughly washed catalyst with standard NaOH (0.01 N) solution and was found to be

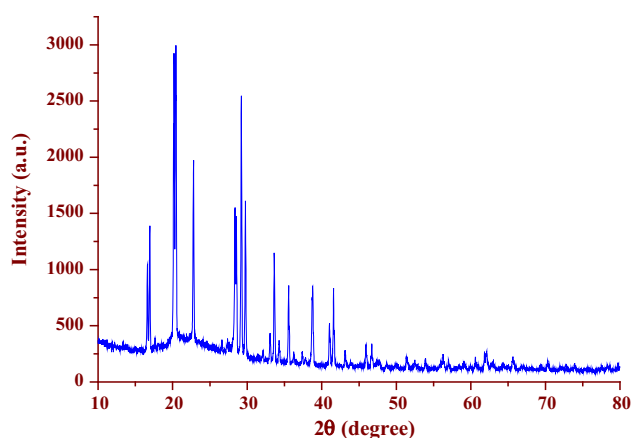


Fig. 6 XRD analysis of catalyst SBPCSA

0.49 meq/g of the support. The concentration of the residual H^+ ion of the recovered catalyst was also measured and found to be small loss of H^+ ion. It signified that SO_3H moiety was tightly anchored with SPBCSA, possibly due to a covalent linkage.

2.2 Chemistry

The synthetic pathways of a series of new acrylonitrile derivatives **3(a–o)** have been shown in Scheme 2. Herein, each series was typically accessed via Knoevenagel condensation between 2-thiopheneacetonitrile (**2**) and appropriately substituted heterocyclic/aromatic aldehydes **1(a–o)** to yield target acrylonitrile derivatives in excellent yields (92–98 %) with high purity. The structural elucidation of the synthesized compounds **3(a–o)** have been established

on the basis of elemental analysis (C, H, N), IR, 1H NMR, ^{13}C NMR and mass spectral analysis. The results for C, H and N analysis were within ± 0.3 % of the theoretical values. The spectral analysis has been in good corroboration with the expected structural framework of the synthesized compounds. All the synthesized compounds showed the absence of the carbonyl peak in the IR spectrum, which confirmed the reaction at the carbonyl moiety. Moreover, all compounds exhibited a characteristic peak for cyano group resonating at around $2200\text{--}2220\text{ cm}^{-1}$. Other characteristic peaks for the different functional groups such as $C=O_{\gamma\text{-pyrone}}$, OH and NO_2 are discussed in experimental section. The 1H NMR spectrum of each compound displayed a sharp singlet at around δ 7.40–8.21 ascribed to the olefinic proton ($H-1'$). Similarly, sharp singlets resonating at around δ 7.25, 7.01, 7.28, 7.23 each integrating for one proton, has been attributed to H-2 protons of γ -pyrone ring of chromones **3a**, **3b**, **3c** and **3d** respectively. Doublet at around δ 7.12–7.39 and 7.26–7.78 have been attributed to H-3' and H-5' protons of thiophene ring and a multiplet at around δ 7.13–7.43 has been attributed to H-4' proton of thiophene ring. ^{13}C NMR spectra, showed a series of signals resonating at around δ 106.86–178.45 which have been assigned to aromatic carbons, peaks resonating at around δ 126.00–137.73 have been ascribed to carbons of thiophene ring. Similarly, peaks resonating at around δ 117.38–119.70 corresponds to $-C\equiv N$ moiety and the signals at δ 178.50, 177.82, 177.09, 177.87 and 178.10 have been attributed to carbonyl group ($C=O_{\gamma\text{-pyrone}}$) of compounds **3a**, **3b**, **3c**, **3d** and **3e**, respectively. Furthermore peaks at δ 107.20–115.49 and 152.12–153.90 corresponds to C-1'' and C-2'', respectively.

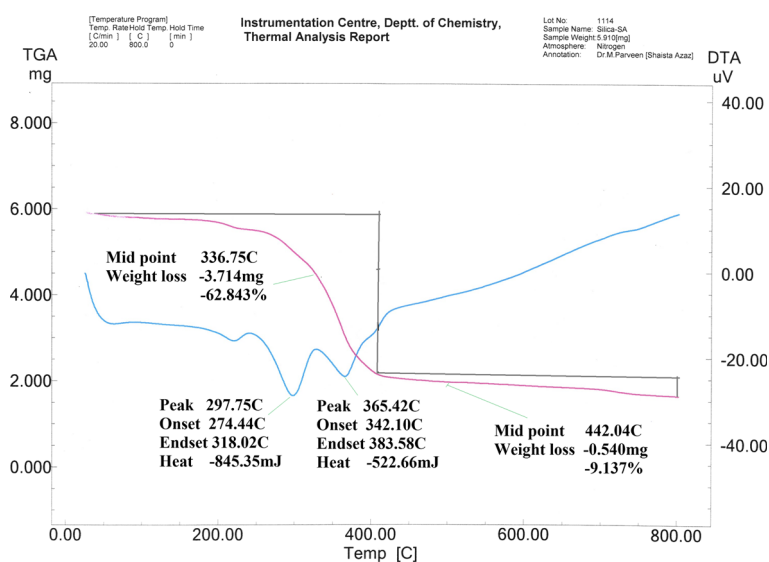
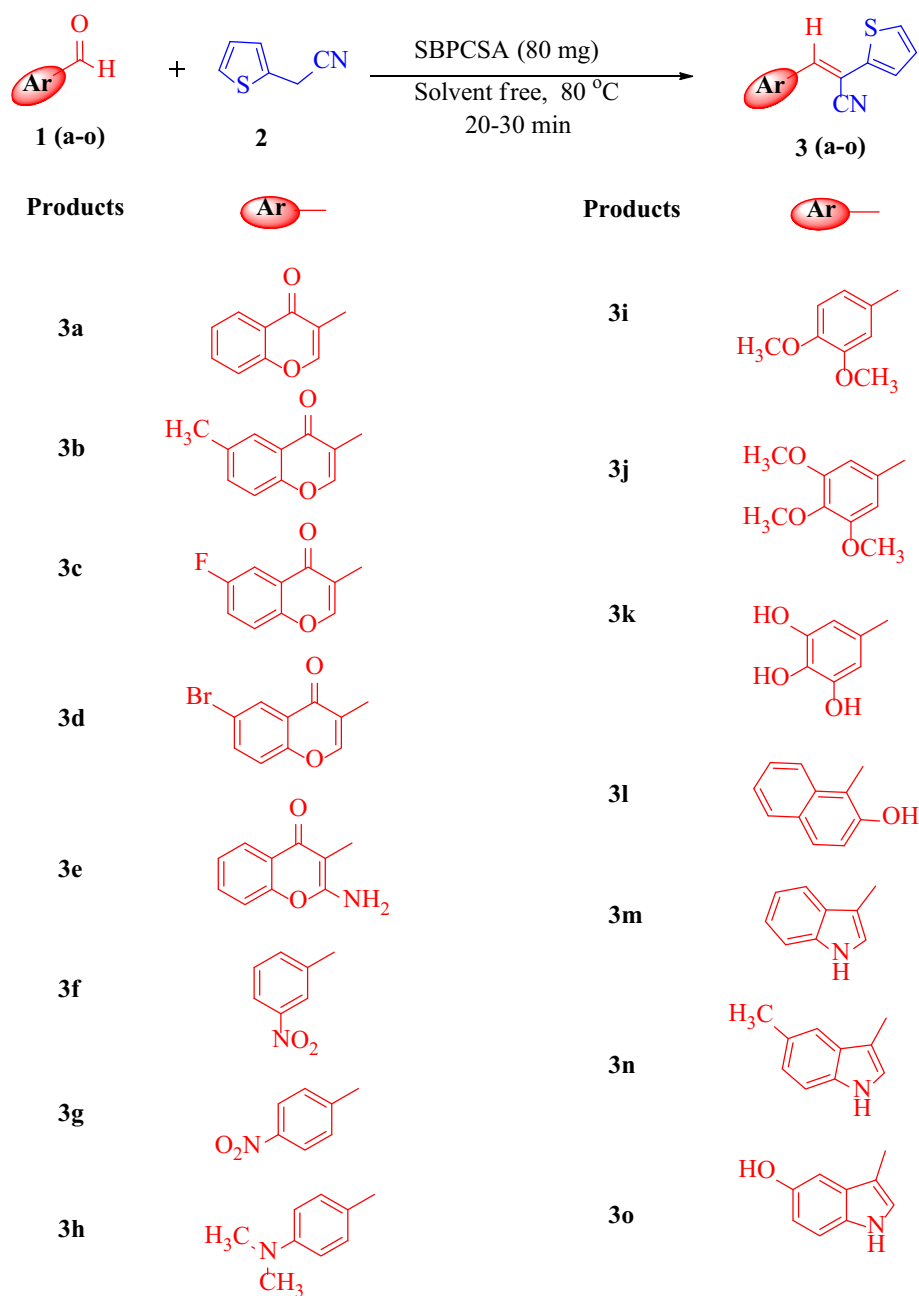


Fig. 7 TGA/DTA analysis of catalyst SBPCSA



Scheme 2 Synthetic scheme for the formation of acrylonitrile derivatives

The mass spectral analysis of the synthesized compounds was also in good conformity with the proposed structures.

In the present study, it was not possible to confirm geometry across C=C on the basis of ^1H NMR analysis. In order to gain some insight into the influence of the electronic interactions on the molecular geometry, we have performed quantum mechanical calculations of the equilibrium geometry of the free molecule. For this purpose we choose compound **3f** for the DFT study. Of the two possible geometrical isomers (*E/Z*) of the compound **3f**, *E*-isomer was

obtained as the sole product. To probe the relative stability of the two possible isomers, MM2 energy-minimization calculations were performed. It was found that the *E*-isomer is stabilized by 12.53 kcal/mol of energy than *Z*-isomer and this energy difference is satisfactory enough to suggest that during the crystallization process, the *E*-isomer gets exclusively crystallized out from the solution. The ground state optimized structure of *E*-isomer interpreted by DFT is shown in Fig. 8, wherein the thiophene part of the molecule is planar with the acrylic moiety, while the nitrophenyl group is

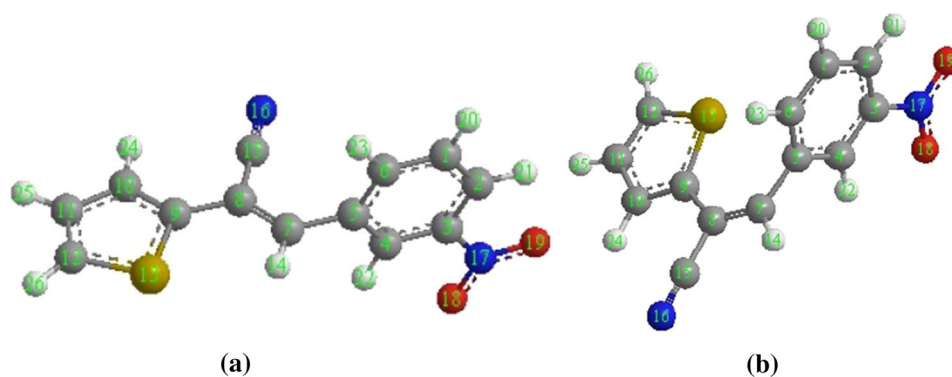


Fig. 8 Ground state optimized structure of **a** (*E*-isomer) and **b** (*Z*-isomer) of compound **3f**

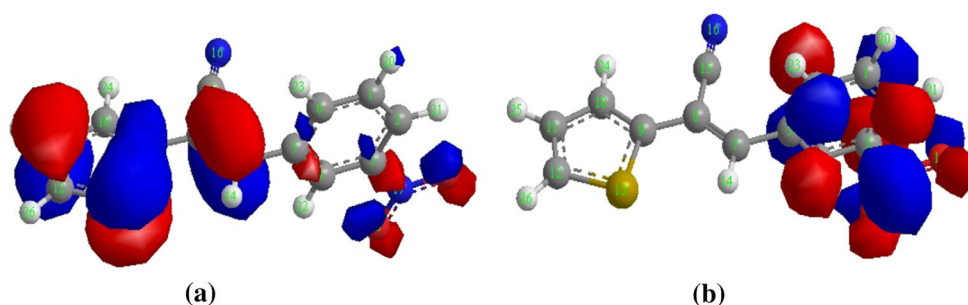


Fig. 9 Electron density distribution in **a** HOMO and **b** LUMO of (*E*-isomer) of compound **3f**

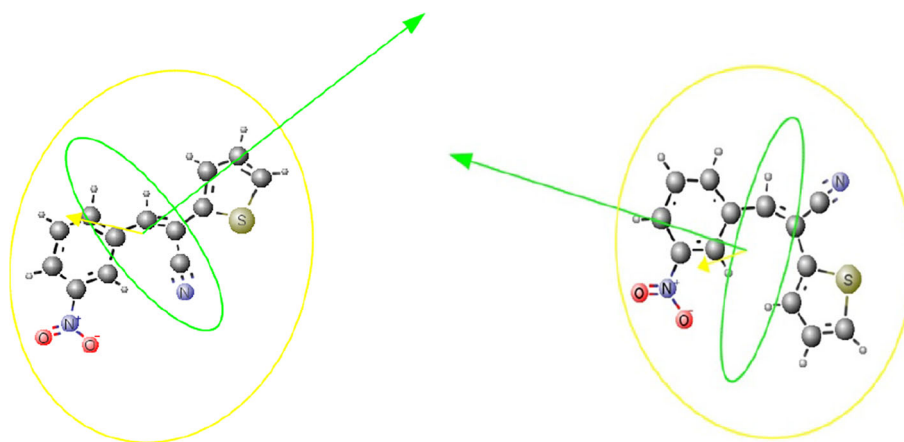
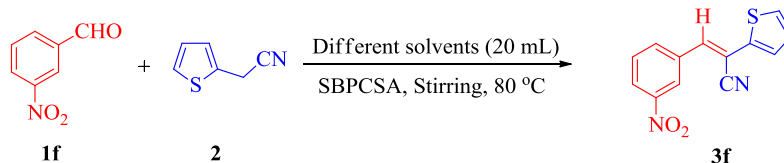


Fig. 10 Dreiding models of the *E* and *Z*-geometrical isomers of the compound **3f**

pushed out of the plane, probably by the electronic interactions between the two lone pairs of sulfur atom of thiophene ring and hydrogen atom (H23) of nitrophenyl ring (:S:-H23). The optimized geometry exhibits the *E*-configuration of the thiophene and nitrophenyl group about the acrylic double bond (Fig. 8). The energies of highest occupied molecular orbital (E_{HOMO}) and lowest unoccupied molecular orbital (E_{LUMO}) and their distributions using DFT-B3LYP/6-311G

were calculated using grid based density functional theory (DFT) at the B3LYP/6-311G basis set level. The calculated energies of HOMO and LUMO were found to be -11.89 and -4.36 eV, respectively, for the optimized *E*-isomer. The energies of HOMO and LUMO, including neighboring orbitals, were all negative, indicating that *E*-isomer is stable. It was observed that the highest occupied molecular orbitals in *E*-isomer is located in the thiophene ring and acrylic

Table 1 Effect of different solvents on model reaction

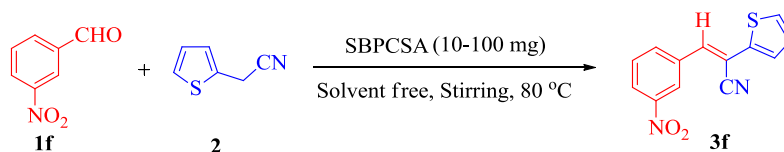
Entry	Solvent	Temp (°C)	Time (h) ^a	Yield (%) ^b
1	MeOH	Reflux	6	70
2	EtOH	Reflux	8	68
3	Water	Reflux	3	66
4	CH ₃ COOH	Reflux	3	75
5	CH ₂ Cl ₂	Reflux	6.5	65
6	DMF	Reflux	7	63
7	Solvent-free	Reflux	20 ^c	98

Reaction condition 3-nitrobenzaldehyde (**1f**, 2 mmol), 2-thiopheneacetonitrile (**2**, 2 mmol), different solvents (20 mL), SBPCSA (80 mg), 80 °C

^a Reaction progress monitored by TLC

^b Isolated yield of products

^c Reaction progress monitored by TLC (entry 7, min)

Table 2 Effect of catalyst loading on model reaction

Entry	Catalyst (mg)	Time (min) ^a	Yield (%) ^b
1	10	120	65
2	20	80	72
3	40	55	79
4	60	40	84
5	80	20	98
6	100	20	98

Reaction condition 3-nitrobenzaldehyde (**1f**, 2 mmol), 2-thiopheneacetonitrile (**2**, 2 mmol), solvent free, SBPCSA (10–100 mg), 80 °C

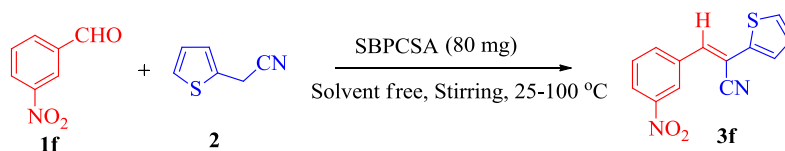
^a Reaction progress monitored by TLC

^b Isolated yield of products

moiety while lowest unoccupied molecular orbitals is mainly localized on the nitro phenyl ring (Fig. 9). *E*-isomer selectivity in the present protocol was further verified on the basis of dreiding energy concept calculated by using ChemAxon, *E* and *Z*-isomers were found to have 63.70 and 92.21 kcal/mol of dreiding energy, respectively. This energy difference of 29.15 kcal/mol is favorable for the selective formation of *E*-isomer (Fig. 10). On the basis of these results it was believed that all the synthesized compounds possess *E*-configuration.

2.3 Optimization of Reaction Conditions

Initially, we focused our study to probe the optimized reaction conditions for the present protocol regarding the choice of solvent, amount of catalyst, temperature of reaction and investigating efficiency of various catalyst on a selected model reaction using 3-nitrobenzaldehyde (**1f**) and 2-thiopheneacetonitrile (**2**) in the presence of SBPCSA to establish the best possible reaction conditions for the synthesis of acrylonitrile **3f**.

Table 3 Effect of temperature on model reaction

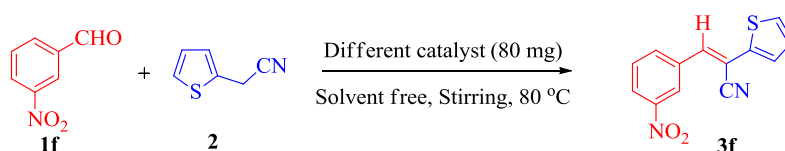
Entry	Temperature (°C)	Time (h) ^a	Yield (%) ^b
1	Room temp	3.0	66
2	40	2.5	72
3	55	2.0	85
4	70	1.0	92
5	80	20 ^c	98
6	100	20 ^c	98

Reaction condition 3-nitrobenzaldehyde (**1f**, 2 mmol), 2-thiopheneacetonitrile (**2**, 2 mmol), solvent free, SBPCSA (80 mg), 25–100 °C

^a Reaction progress monitored by TLC

^b Isolated yield of products

^c Reaction progress monitored by TLC (entry 5–6, min)

Table 4 Comparison of the efficiency of SBPCSA with different catalysts on the model reaction

Entry	Catalyst	Time h/(min) ^a	Yield (%) ^b
1	–	300	Traces
2	SiO ₂	240	40
3	SiO ₂ –NH ₄ SO ₄	80	74
4	SiO ₂ –Cl	100	70
5	SiO ₂ –H ₂ SO ₄	65	76
6	SiO ₂ –HClO ₄	48	81
7	NH ₂ SO ₃ H	55	89
8	SBNPU	60	83
9	SBPCSA	20	98

Reaction condition 3-nitrobenzaldehyde (**1f**, 2 mmol), 2-thiopheneacetonitrile (**2**, 2 mmol), solvent free, different catalysts (80 mg), 80 °C

^a Reaction progress monitored by TLC

^b Isolated yield of products

2.3.1 Effect of Different Reaction Media

In order to optimize the reaction conditions we first probed the effect of solvents by carrying out the model reaction in various conventional organic solvent systems. Initially the model reaction was performed in organic solvents like MeOH and EtOH (Table 1, entries 1–2) a moderate yield of

the product 70 and 68 %, respectively, was obtained after a stretched time period (6–8 h). This moderate yield can be attributed to the nucleophilic nature of these solvents, which may force the reaction to undergo nucleophilic competition between these solvents (MeOH, EtOH) and active methylene (2-thiopheneacetonitrile) for electrophilic carbon of carbonyl group that will eventually results in

Table 5 Synthesis of acrylonitrile derivatives **3(a–o)**

Product	Structure	Reaction in presence of piperidine ^a		Reaction in presence of catalyst ^b		M.P °C
		Time yield		Time yield		
		(h)	(%)	(min)	(%)	
3a		6.0	69	20	96	213–214
3b		7.5	72	24	94	198–200
3c		6.0	70	20	98	211
3d		7.0	70	22	96	220
3e		7.5	68	25	94	230–232
3f		6.5	70	20	98	150
3g		6.0	72	20	96	125
3h		7.5	67	25	98	132
3i		8.0	60	26	98	136
3j		8.0	68	30	95	149

Table 5 continued

Product	Structure	Reaction in presence of piperidine ^a		Reaction in presence of catalyst ^b		M.P °C
		Time yield		Time yield		
		(h)	(%)	(min)	(%)	
3k		8.0	62	26	92	158
3l		7.0	60	30	94	132
3m		6.0	65	20	98	195
3n		6.5	62	22	94	198
3o		7.0	68	24	95	210

^a Reaction conditions Differently substituted heterocyclic/aromatic aldehydes **1(a–o)** with 2-thiopheneacetonitrile (**2**) under reflux in ethanol in the presence of piperidine (5 mol%)

^b Reaction conditions Differently substituted heterocyclic/aromatic aldehydes **1(a–o)** with 2-thiopheneacetonitrile (**2**) in presence of SBPCSA (80 mg) at 80 °C

lower yield of the desired product (**3f**), whereas in water (Table 1, entry 3) the product was obtained in 66 % yield after refluxing for 3 h. This apparent drop in reaction time in water is believed to be due to the hydrogen bonding between the water and carbonyl group of the substrate, which may stabilize the intermediate structure during the formation of product. In CH_3COOH , the yield of the desired product increased significantly (75 %) with reduced reaction time (Table 1, entry 4). This enhancement in yield in CH_3COOH solvent is probably due to its ability to trigger the carbonyl group of the reactants by electromeric effect, thereby enhancing the electrophilicity of carbon,

rendering it more feasible for nucleophilic attack by the active methylene 2-thiopheneacetonitrile. However, when the reaction was carried out in non-coordinating solvents like CH_2Cl_2 and DMF no further significant increase in the yield of the product was observed in comparison to CH_3COOH after a stretched reaction time (Table 1, entries 5 and 6). Moreover, when the model reaction was explored in solvent-free condition, there was remarkable increase in the yield of the product (98 %) with prominent fall in reaction time (20 min) (Table 1, entry 7). It is evident from the result that nature of solvent plays a crucial role in the degree of selectivity of the desired product (**3f**). In view of

the above results, it was concluded that solvent-free condition is the best condition for the synthesis of acrylonitrile derivatives.

2.3.2 Effect of Catalyst Loading

To achieve the optimum concentration of the catalyst for the present protocol, the model reaction was investigated at different concentrations i.e., 10, 20, 40, 60, 80 and 100 mg (Table 2) of the catalyst SBPCSA at 80 °C under solvent-free condition and the results were noted in terms of reaction time and yield. It was inferred from Table 2 that with every subsequent increase in concentration of catalyst from 10 to 80 mg, there has been a noteworthy improvement in the yield from 65 to 98 %, with prominent drop in reaction time from 120 to 20 min (entries 1–5, Table 2). However, further increase in the concentration of the catalyst (>80 mg) did not have any significant effect on the reaction. Thus, it can be concluded from the above results that 80 mg of the catalyst is adequate to gain the optimum yield in the shortest reaction time under neat conditions at 80 °C, therefore 80 mg of the catalyst was selected for further studies.

2.3.3 Effect of Temperature

To optimize the reaction temperature, the model reaction was carried out at different temperatures in presence of catalyst SBPCSA (Table 3). The reaction was initially tested at room temperature and does not give satisfactory yield of desired product **3f** (Table 3, entry 1). It was observed that the increase in temperature from 25 to 80 °C, has a noteworthy effect on the model reaction with increase in the yield of desired product **3f** (66–98 %) with the prominent decrease in the reaction time (Table 3, entry 1–5). However, a further increase in the temperature from 80 to 100 °C did not show any further increase in the yield of the product **3f** (Table 3, entry 6). Thus, keeping in view the above optimized reaction conditions; 80 °C was preferred as the optimal temperature for all the reactions in the presence of 80 mg of SBPCSA under solvent-free conditions.

2.3.4 Comparison of Efficacy of Silica Bonded *N*-(Propylcarbamoyl)sulfamic acid (SBPCSA)

A comparative study of a variety of catalysts was conducted to probe the superiority of our catalyst SBPCSA (Table 4). The model reaction was first investigated without catalyst and it was found that the reaction took prolonged reaction time with trace of the yield. Further the

reaction was tested with blank-SiO₂, SiO₂–NH₄SO₄ and SiO₂–Cl, moderate yield of products were obtain with prolonged time period (Table 4, entries 2–4). When the reaction was carried out in presence of SiO₂–H₂SO₄ and SiO₂–HClO₄ there was an increase in the yield of product with decrease in the reaction time (Table 4, entries 5, 6). To obtain better yield in less reaction time we further use sulfamic acid and SBNPU to catalyze the reaction and found better results in term of yield and time (Table 4, entries 7, 8). Moreover, when the model reaction was probed with SBPCSA the yield of product (**3f**) increased exponentially (98 %) with a prominent dip in reaction time (20 min).

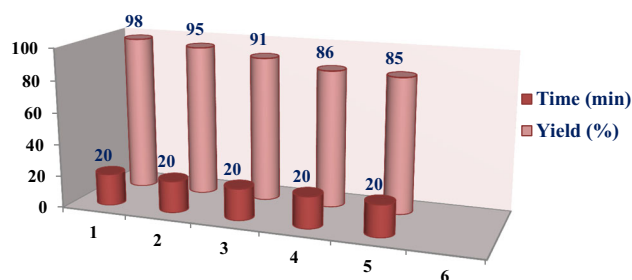


Fig. 11 Recyclability of the catalyst SBPCSA for the model reaction

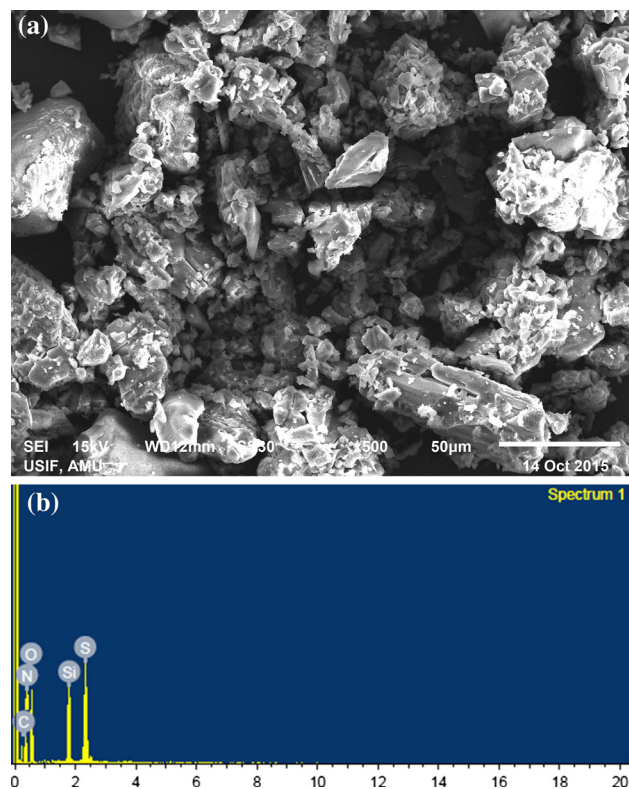


Fig. 12 SEM and EDX analysis of recovered catalyst SBPCSA

Using these optimized reaction conditions as discussed above, the efficacy of this approach was explored for a wide variety of heterocyclic/aromatic aldehydes possessing electron-withdrawing and electron-donating groups for the synthesis of acrylonitrile derivatives in excellent yields (92–98 %) (Table 5). In the present study a comparative study has also been carried out for the present protocol with the conventional Knoevenagel condensation by carrying out the reaction of aldehydes with 2-thiopheneacetonitrile under reflux in ethanol in the presence of 5 mol% of piperidine. It was observed that the reaction took prolonged reaction time (6–8 h) for completion with moderate yield (60–72 %). The results revealed that employing SBPCSA in the present protocol enhances selectivity and product conversion thus, proves beneficial over the conventional method for the synthesis of acrylonitrile in terms of yield and reaction times.

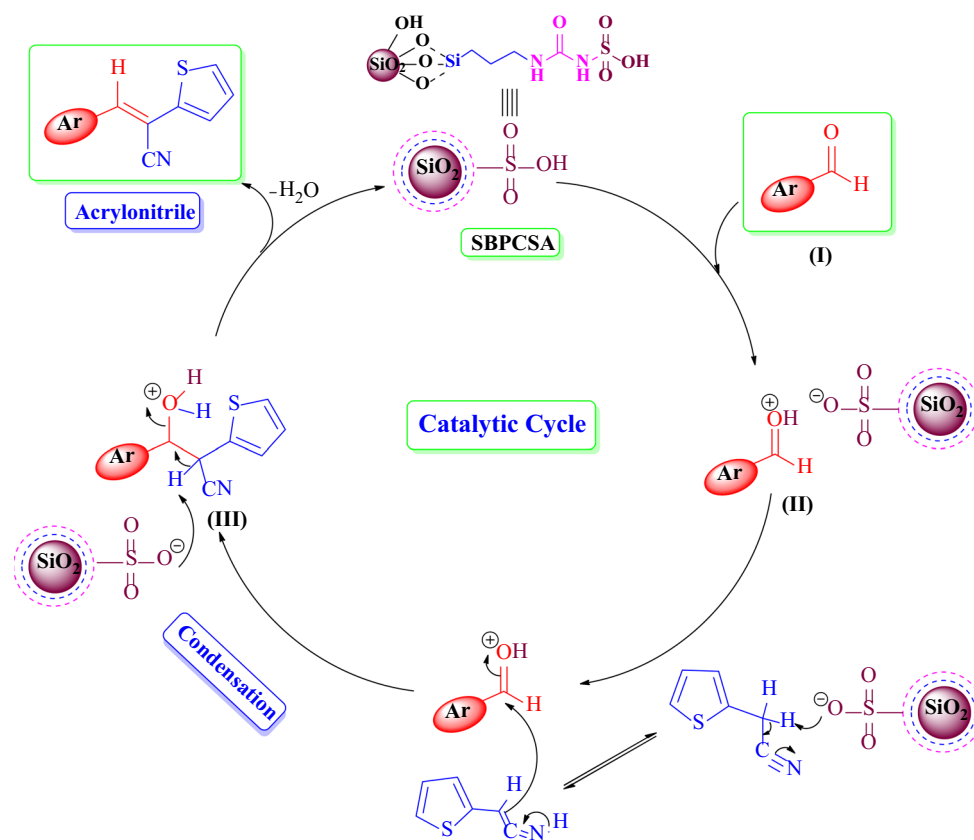
2.4 Recyclability of the Catalyst

The reusability of the catalyst was also explored for the selected model reaction in order to reduce the cost of the

process. After completion of the reaction, catalyst was removed by simple filtration, washed with ethanol and dried under vacuum at 80 °C for 6 h and was further tested up to four more reaction cycles. Recycling and reuse of the catalyst showed minimal decreases in yields (Fig. 11). Although the reaction rate get decreased gradually with repetition of the reaction cycle, however we succeeded in obtaining the desired product **3f** in satisfactory yield (85 %) even after 5th repetition of the model reaction without any addition of the fresh catalyst (Fig. 11). To ascertain the variation in morphological features of the recovered catalyst, we carry out its SEM-EDX analysis (Fig. 12). It was observed that the composition of the catalytic system was almost consistent with the fresh catalyst and also there was no significant change observed in the morphology of the catalyst as compared to the fresh catalyst.

2.5 Reaction Mechanism

A plausible mechanistic pathway is proposed in Scheme 3, to illustrate the synthesis of acrylonitrile derivatives catalyzed by SBPCSA. The initial step is assumed to be the



Scheme 3 Plausible mechanistic pathway for the synthesis of acrylonitrile derivatives

protonation of formyl group (–CHO) of substrates (**I**) by protic SBPCSA catalyst to form intermediate (**II**), which facilitates the nucleophilic attack of 2-thiopheneacetonitrile to promote the formation of C–C bond to yield intermediate (**III**). The subsequent elimination of H₂O molecule from intermediate (**III**) promoted by catalyst SBPCSA eventually yielded target compound followed by regeneration of the catalyst.

3 Conclusions

The present protocol reports a convenient, eco-friendly and sustainable approach for the synthesis of *E*-acrylonitrile derivatives **3(a–o)** in excellent yields (92–98 %) by employing SBPCSA as a catalyst. This solvent-free, green synthetic procedure eliminates the use of toxic solvents and thus makes it distinctive one in organic synthesis. The protocol offers mild reaction conditions, shorter reaction time, high purity, operational simplicity, cleaner reaction profile, enhanced reaction rates and easy workup. The catalyst SBPCSA is easily synthesized and can be used up to five cycles without any significant loss in catalytic activity. We believe that this synthetic approach provides a better scope for the synthesis of acrylonitrile analogues and will be a more practical alternative to the other existing methods.

4 Experimental

4.1 Materials and General Methods

Chemicals were purchased from Merck and Sigma-Aldrich as ‘synthesis grade’ and used without further purification. Elemental analysis (C, H, N) was conducted using Carlo Erba analyzer model 1108. Melting points were determined on a Kofler apparatus and are uncorrected. The IR spectra were recorded with a Shimadzu IR-408 Perkin-Elmer 1800 instrument (FTIR), and the values are given in cm⁻¹. ¹H NMR and ¹³C NMR spectra were run in DMSO-*d*₆ on a Bruker Avance-II 400 MHz instrument with TMS as an internal standard and J values measured in Hertz. Chemical shifts are reported in ppm (δ) relative to TMS. Mass spectra were recorded on a JEOLD-300 mass spectrometer. X-ray diffractogram (XRD) of the catalyst were recorded in the 2θ range of 20°–80° with a scan rate of 41 min⁻¹ on a Shimadzu-6100 X-ray diffractometer with Ni-filtered Cu Kα radiation at a wavelength of 1.54060 Å. The scanning electron microscope (SEM-EDX) analysis was obtained using a JEOL (JSM-6510) equipped with an energy dispersive X-ray spectrometer at different magnification. TGA has been carried out with DTG-60H (Simultaneous DTA-TG Apparatus), Shimadzu instrument. Thin layer

chromatography (TLC) glass plates (20 × 5 cm) were coated with silica gel G (Merck) using benzene-acetone (8:2) mixture as mobile phase and exposed to iodine vapors to check the homogeneity as well as the progress of the reaction.

4.2 Synthesis of Catalyst

4.2.1 Preparation of 3-Chloropropylsilica [60]

In a typical procedure 5 mL (25 mmol) of (3-chloropropyl)-trimethoxysilane was dissolved in 100 mL of dried toluene. 5 g of SiO₂ was added to this mixture and the solution was stirred for 18 h at 60 °C. Then the solid residue was filtered, washed with toluene and dried in vacuum.

4.2.2 Preparation of Urea Functionalized Propylsilica

The synthesized chloropropyl silica (3 g) was added to a solution of urea (1.2 g, 20 mmol) in ethanol (50 mL) in a round-bottom flask and the mixture was stirred under reflux condition for 8 h. The obtained solid was then filtered and washed with ethanol followed by drying at 80 °C for 12 h.

4.2.3 Preparation of Silica Bonded *N*-(Propylcarbamoyl)sulfamic acid (SBPCSA) [61]

To a mixture of urea functionalized propyl silica (2.5 g) in CH₂Cl₂ (20 mL), chlorosulphonic acid (1.2 mL) was added drop wise at room temperature over a period of 30 min. After addition was completed, the mixture was further stirred for 90 min and HCl gas evolution was monitored with a pH paper indicator. The mixture was filtered and washed with CH₂Cl₂ (50 mL) and dried in vacuum at 80 °C to afford SBPCSA.

4.3 General Procedure for the Synthesis of Acrylonitrile Derivatives

To a mixture of substituted aromatic aldehydes **1(a–o)** (2 mmol) and 2-thiopheneacetonitrile **2** (2 mmol), 80 mg of SBPCSA was added and the reaction mixture was heated on an oil bath at 80 °C for (20–30 min) with stirring. After completion of the reaction as evident from thin layer chromatography (TLC), the reaction mixture was diluted with ethanol and filtered off to recover the catalyst for further use in catalytic cycles. The filtrate was evaporated under reduced pressure to obtain the product. The crude product was further purified by crystallization from appropriate solvent to afford the pure product **3(a–o)**.

4.4 Spectral Characterization

4.4.1 (*E*)-3-(4-Oxo-4H-chromen-3-yl)-2-(thiophen-2-yl)acrylonitrile (**3a**)

Yellow crystalline solid, yield 96 %, m.p. 213–214 °C, Analytical cal. C₁₆H₉NO₂S: C, 68.80; H, 3.25; N, 5.01; found: C, 68.77; H, 3.26; N, 5.03. IR (KBr cm⁻¹): 2219 (C≡N), 1652 (C=O_{γ-pyrone}), 1612 (C=C_{γ-pyrone}), 1560, 1462 (C=C_{aromatic}). ¹H NMR (400 MHz, DMSO-*d*₆, δ, ppm): 7.25 (s, 1H, H-2), 8.01 (d, 1H, H-5), 7.45 (m, 1H, H-6), 7.58 (m, 1H, H-7), 7.58 (d, 1H, H-8), 7.40 (s, 1H, =CH_{olifinic}), 7.38 (d, 1H, H-3'), 7.20 (m, 1H, H-4'), 7.70 (d, 1H, H-5'). ¹³C NMR (100 MHz, DMSO-*d*₆, δ, ppm): 150.12 (C-2), 118.50 (C-3), 178.45 (C-4), 124.82 (C-5), 123.83 (C-6), 135.51 (C-7), 116.82 (C-8), 125.54 (C-4a), 152.44 (C-8a), 136.05 (C-2'), 127.42 (C-3'), 127.15 (C-4'), 131.51 (C-5'), 110.45 (C-1'), 152.84 (C-2'), 178.50 (C=O), 117.91 (CN). MS (EI): (m/z) 279.04 [M⁺].

4.4.2 (*E*)-3-(6-Methyl-4-oxo-4H-chromen-3-yl)-2-(thiophen-2-yl)acrylonitrile (**3b**)

Yellow solid, yield 94 %, m.p. 198–200 °C, Analytical cal. C₁₇H₁₁NO₂S: C, 69.61; H, 3.78; N, 4.77; found: C, 69.60; H, 3.79; N, 4.74. IR (KBr cm⁻¹): 2215 (C≡N), 1658 (C=O_{γ-pyrone}), 1618 (C=C_{γ-pyrone}), 1558, 1461 (C=C_{aromatic}). ¹H NMR (400 MHz, DMSO-*d*₆, δ, ppm): 7.01 (s, 1H, H-2), 7.80 (s, 1H, H-5), 7.84 (m, 1H, H-7), 7.58 (d, 1H, H-8), 2.38 (s, 3H, CH₃), 7.45 (s, 1H, =CH_{olifinic}), 7.39 (d, 1H, H-3'), 7.22 (m, 1H, H-4'), 7.75 (d, 1H, H-5'). ¹³C NMR (100 MHz, DMSO-*d*₆, δ, ppm): 150.56 (C-2), 118.96 (C-3), 177.82 (C-4), 123.87 (C-5), 133.92 (C-6), 137.43 (C-7), 113.12 (C-8), 21.81 (CH₃), 125.77 (C-4a), 152.32 (C-8a), 134.89 (C-2'), 127.53 (C-3'), 127.01 (C-4'), 131.84 (C-5'), 115.49 (C-1'), 154.80 (C-2'), 177.82 (C=O), 117.38 (CN). MS (EI): (m/z) 293.05 [M⁺].

4.4.3 (*E*)-3-(6-Fluoro-4-oxo-4H-chromen-3-yl)-2-(thiophen-2-yl)acrylonitrile (**3c**)

Yellow crystalline solid, yield 98 %, m.p. 211 °C, Analytical cal. C₁₆H₈FNO₂S: C, 64.64; H, 2.71; N, 4.71; found: C, 64.62; H, 2.70; N, 4.74. IR (KBr cm⁻¹): 2219 (C≡N), 1662 (C=O_{γ-pyrone}), 1620 (C=C_{γ-pyrone}), 1559, 1464 (C=C_{aromatic}). ¹H NMR (400 MHz, DMSO-*d*₆, δ, ppm): 7.28 (s, 1H, H-2), 7.80 (s, 1H, H-5), 7.68 (d, 1H, H-7), 7.50 (d, 1H, H-8), 7.48 (s, 1H, =CH_{olifinic}), 7.36 (d, 1H, H-3'), 7.20 (m, 1H, H-4'), 7.73 (d, 1H, H-5'). ¹³C NMR (100 MHz, DMSO-*d*₆, δ, ppm): 149.61 (C-2), 118.02 (C-3), 177.00 (C-4), 109.81 (C-5), 161.84 (C-6), 123.52 (C-7), 121.73 (C-8), 125.22 (C-4a), 152.91 (C-8a), 136.73 (C-2'), 127.26 (C-3'), 128.84 (C-4'), 131.03 (C-5'), 112.22

(C-1'), 152.12 (C-2'), 177.09 (C=O), 118.13 (CN). MS (EI): (m/z) 297.03 [M⁺].

4.4.4 (*E*)-3-(6-Bromo-4-oxo-4H-chromen-3-yl)-2-(thiophen-2-yl)acrylonitrile (**3d**)

Yellow solid, yield 96 %, m.p. 220 °C, Analytical cal. C₁₆H₈BrNO₂S: C, 53.65; H, 2.25; N, 3.91; found: C, 53.63; H, 2.26; N, 3.93. IR (KBr cm⁻¹): 2214 (C≡N), 1665 (C=O_{γ-pyrone}), 1627 (C=C_{γ-pyrone}), 1554, 1467 (C=C_{aromatic}). ¹H NMR (400 MHz, DMSO-*d*₆, δ, ppm): 7.23 (s, 1H, H-2), 7.94 (s, 1H, H-5), 7.78 (d, 1H, H-7), 7.10 (d, 1H, H-8), 8.09 (s, 1H, =CH_{olifinic}), 7.38 (d, 1H, H-3'), 7.20 (m, 1H, H-4'), 7.63 (d, 1H, H-5'). ¹³C NMR (100 MHz, DMSO-*d*₆, δ, ppm): 149.90 (C-2), 119.08 (C-3), 177.81 (C-4), 135.82 (C-5), 124.8 (C-6), 143.51 (C-7), 118.70 (C-8), 127.25 (C-4a), 157.91 (C-8a), 136.90 (C-2'), 128.26 (C-3'), 129.81 (C-4'), 131.82 (C-5'), 107.20 (C-1'), 153.15 (C-2'), 177.87 (C=O), 118.90 (CN). MS (EI): (m/z) 358.94 [M⁺].

4.4.5 (*E*)-3-(2-Amino-4-oxo-4H-chromen-3-yl)-2-(thiophen-2-yl)acrylonitrile (**3e**)

Yellow solid, yield 94 %, m.p. 230–232 °C, Analytical cal. C₁₆H₁₀N₂O₂S: C, 65.29; H, 3.42; N, 9.52; found: C, 65.26; H, 3.44; N, 9.53. IR (KBr cm⁻¹): 2220 (C≡N), 1651 (C=O_{γ-pyrone}), 1614 (C=C_{γ-pyrone}), 1565, 1461 (C=C_{aromatic}). ¹H NMR (400 MHz, DMSO-*d*₆, δ, ppm): 8.5 (s, 2H, N-H, D₂O exchangeable), 7.75 (d, 1H, H-5), 7.48 (m, 1H, H-6), 7.58 (m, 1H, H-7), 7.56 (d, 1H, H-8), 8.12 (s, 1H, =CH_{olifinic}), 7.36 (d, 1H, H-3'), 7.18 (m, 1H, H-4'), 7.70 (d, 1H, H-5'). ¹³C NMR (100 MHz, DMSO-*d*₆, δ, ppm): 168.12 (C-2), 106.88 (C-3), 178.14 (C-4), 125.80 (C-5), 124.81 (C-6), 135.85 (C-7), 117.02 (C-8), 124.51 (C-4a), 158.45 (C-8a), 136.33 (C-2'), 126.42 (C-3'), 127.71 (C-4'), 131.73 (C-5'), 114.28 (C-1'), 153.56 (C-2'), 178.10 (C=O), 118.06 (CN). MS (EI): (m/z) 294.05 [M⁺].

4.4.6 (*E*)-3-(3-Nitrophenyl)-2-(thiophen-2-yl)acrylonitrile (**3f**)

Yellow crystalline solid, yield 98 %, m.p. 150 °C, Analytical cal. C₁₃H₈N₂O₂S: C, 60.93; H, 3.15; N, 10.93; found: C, 60.90; H, 3.16; N, 10.95. IR (KBr cm⁻¹): 2218 (C≡N), 1562, 1440 (C=C_{aromatic}), 1518, 1320 (NO₂). ¹H NMR (400 MHz, DMSO-*d*₆, δ, ppm): 8.50 (s, 1H, H-2), 7.48 (d, 1H, H-4), 8.26–8.31 (t, 1H, H-5), 7.47–7.48 (d, 1H, H-6), 7.67 (s, 1H, =CH_{olifinic}), 7.12–7.14 (d, 1H, H-3'), 7.39–7.43 (t, 1H, H-4'), 7.26 (d, 1H, H-5'). ¹³C NMR (100 MHz, DMSO-*d*₆, δ, ppm): 136.51 (C-1), 122.12 (C-2), 147.35 (C-3), 124.82 (C-4), 129.26 (C-5), 136.11 (C-6),

135.21 (C-2'), 126.72 (C-3'), 128.90 (C-4'), 130.18 (C-5'), 107.68 (C-1'), 152.44 (C-2''), 118.34 (CN). MS (EI): (m/z) 256.03 [M⁺].

4.4.7 (*E*)-3-(4-Nitrophenyl)-2-(thiophen-2-yl)acrylonitrile (**3g**)

Yellow crystalline solid, yield 96 %, m.p. 125 °C, Analytical cal. C₁₃H₈N₂O₂S: C, 60.93; H, 3.15; N, 10.93; found: C, 60.90; H, 3.17; N, 10.94. IR (KBr cm⁻¹): 2214 (C≡N), 1560, 1445 (C=C_{aromatic}), 1512, 1322 (NO₂). ¹H NMR (400 MHz, DMSO-*d*₆, δ, ppm): 8.0 (dd, 2H, H-2 and H-6), 8.15 (dd, 2H, H-4 and H-6), 7.41 (s, 1H, =CH_{olifinic}), 7.20 (d, 1H, H-3'), 7.17 (m, 1H, H-4'), 7.60 (d, 1H, H-5'). ¹³C NMR (100 MHz, DMSO-*d*₆, δ, ppm): 141.04 (C-1), 128.51 (C-2 and C-6), 122.80 (C-3 and C-5), 157.81 (C-4), 136.61 (C-2'), 126.62 (C-3'), 128.34 (C-4'), 131.52 (C-5'), 108.26 (C-1''), 153.18 (C-2''), 119.70 (CN). MS (EI): (m/z) 256.03 [M⁺].

4.4.8 (*E*)-3-(4-(Dimethylamino)phenyl)-2-(thiophen-2-yl)acrylonitrile (**3h**)

Brown crystalline solid, yield 98 %, m.p. 132 °C, Analytical cal. C₁₅H₁₄N₂S: C, 70.83; H, 5.55; N, 11.01; found: C, 70.80; H, 5.56; N, 11.03; IR (KBr cm⁻¹): 2218 (C≡N), 1567, 1445 (C=C_{aromatic}). ¹H NMR (400 MHz, DMSO-*d*₆, δ, ppm): 7.62 (dd, 2H, H-2 and H-6), 6.82 (dd, H-3 and H-5), 8.02 (s, 1H, =CH_{olifinic}), 7.24 (d, 1H, H-3'), 7.18 (m, 1H, H-4'), 7.54 (d, 1H, H-5'), 3.11 (s, 6H, CH₃ × 2). ¹³C NMR (100 MHz, DMSO-*d*₆, δ, ppm): 124.01 (C-1), 128.50 (C-2 and C-6), 112.32 (C-3 and C-5), 151.85 (C-4), 137.73 (C-2'), 126.00 (C-3'), 127.31 (C-4'), 137.73 (C-5'), 108.10 (C-1''), 153.80 (C-2''), 118.42 (CN), 42.15 (CH₃). MS (EI): (m/z) 254.09 [M⁺].

4.4.9 (*E*)-3-(3,4-Dimethoxyphenyl)-2-(thiophen-2-yl)acrylonitrile (**3i**)

Pale yellow solid, yield 98 %, m.p. 136 °C, Analytical cal. C₁₅H₁₃NO₂S: C, 66.40; H, 4.83; N, 5.16; found: C, 66.41; H, 4.80; N, 5.18. IR (KBr cm⁻¹): 2215 (C≡N), 1560, 1445 (C=C_{aromatic}). ¹H NMR (400 MHz, DMSO-*d*₆, δ, ppm): 7.82 (s, 1H, H-2), 7.1 (d, 1H, H-5), 7.76 (d, 1H, H-6), 7.45 (s, 1H, =CH_{olifinic}), 7.39 (d, 1H, H-3'), 7.20 (m, 1H, H-4'), 7.68 (d, 1H, H-5'), 3.86 (s, 6H, OCH₃ × 2). ¹³C NMR (100 MHz, DMSO-*d*₆, δ, ppm): 129.21 (C-1), 112.61 (C-2), 149.83 (C-3), 148.84 (C-4), 117.35 (C-5), 123.80 (C-6), 135.05 (C-2'), 127.91 (C-3'), 128.73 (C-4'), 132.94 (C-5'), 108.08 (C-1''), 153.42 (C-2''), 118.20 (CN), 56.21 (CH₃). MS (EI): (m/z) 271.07 [M⁺].

4.4.10 (*E*)-2-(Thiophen-2-yl)-3-(3,4,5-trimethoxyphenyl)acrylonitrile (**3j**)

Yellow crystalline solid, yield 95 %, m.p. 149 °C, Analytical cal. C₁₆H₁₅NO₃S: C, 63.77; H, 5.02; N, 4.65; found: C, 63.75; H, 5.05; N, 4.64. IR (KBr cm⁻¹): 2212 (C≡N), 1562, 1449 (C=C_{aromatic}). ¹H NMR (400 MHz, DMSO-*d*₆, δ, ppm): 7.12 (s, 2H, H-2 and H-6), 7.97 (s, 1H, =CH_{olifinic}), 7.33 (d, 1H, H-3'), 7.21 (m, 1H, H-4'), 7.78 (d, 1H, H-5'), 3.89 (s, 9H, OCH₃ × 3). ¹³C NMR (100 MHz, DMSO-*d*₆, δ, ppm): 128.21 (C-1), 107.62 (C-2 and C-6), 154.84 (C-3 and C-5), 138.86 (C-4), 135.94 (C-2'), 127.02 (C-3'), 128.90 (C-4'), 131.91 (C-5'), 108.22 (C-1''), 152.12 (C-2''), 117.90 (CN), 56.51 (CH₃). MS (EI): (m/z) 301.08 [M⁺].

4.4.11 (*E*)-2-(Thiophen-2-yl)-3-(3,4,5-trihydroxyphenyl)acrylonitrile (**3k**)

Yellow solid, yield 92 %, m.p. 158 °C, Analytical cal. C₁₃H₉NO₃S: C, 60.22; H, 3.50; N, 5.40; found: C, 60.20; H, 3.53; N, 5.39. IR (KBr cm⁻¹): 2214 (C≡N), 1556, 1448 (C=C_{aromatic}). ¹H NMR (400 MHz, DMSO-*d*₆, δ, ppm): 7.42 (s, 2H, H-2 and H-6), 8.00 (s, 1H, =CH_{olifinic}), 7.32 (d, 1H, H-3'), 7.13 (m, 1H, H-4'), 7.54 (d, 1H, H-5'), 5.35 (s, 3H, -OH × 3, D₂O-exchangeable). ¹³C NMR (100 MHz, DMSO-*d*₆, δ, ppm): 131.24 (C-1), 107.41 (C-2), 148.80 (C-3), 134.54 (C-4), 146.32 (C-5), 106.86 (C-6), 135.81 (C-2'), 127.85 (C-3'), 127.90 (C-4'), 131.08 (C-5'), 108.45 (C-1''), 152.44 (C-2''), 118.22 (CN). MS (EI): (m/z) 259.03 [M⁺].

4.4.12 (*E*)-3-(2-Hydroxynaphthalen-1-yl)-2-(thiophen-2-yl)acrylonitrile (**3l**)

Bright yellow solid, yield 94 %, m.p. 132 °C, Analytical cal. C₁₇H₁₁NOS: C, 73.62; H, 4.00; N, 5.05; found: C, 73.62; H, 4.03; N, 5.02. IR (KBr cm⁻¹): 2212 (C≡N), 1565, 1448 (C=C_{aromatic}). ¹H NMR (400 MHz, DMSO-*d*₆, δ, ppm): 7.69 (d, 1H, H-3), 7.90 (d, 1H, H-4), 7.62 (m, 1H, H-5), 7.53 (m, 1H, H-6), 7.95 (m, 1H, H-7), 8.40 (d, 1H, H-8), 8.21 (s, 1H, =CH_{olifinic}), 7.38 (d, 1H, H-3'), 7.20 (m, 1H, H-4'), 7.68 (d, 1H, H-5'), 5.35 (s, 1H, -OH, D₂O-exchangeable). ¹³C NMR (100 MHz, DMSO-*d*₆, δ, ppm): 107.50 (C-1), 158.02 (C-2), 110.89 (C-3), 127.01 (C-4), 127.22 (C-5), 123.90 (C-6), 128.21 (C-7), 115.56 (C-8), 124.96 (C-9), 141.11 (C-10), 135.91 (C-2'), 126.41 (C-3'), 127.90 (C-4'), 131.18 (C-5'), 108.08 (C-1''), 153.41 (C-2''), 118.20 (CN). MS (EI): (m/z) 227.04 [M⁺].

4.4.13 (*E*)-3-(1*H*-Indol-3-yl)-2-(thiophen-2-yl)acrylonitrile (**3m**)

Yellow crystalline solid, yield 98 %, m.p. 195 °C, Analytical cal. C₁₅H₁₀N₂S: C, 71.97; H, 4.03; N, 11.19; found:

C, 71.97; H, 4.03; N, 11.19. IR (KBr cm^{-1}): 2212 ($\text{C}\equiv\text{N}$), 1550, 1445 ($\text{C}=\text{C}_{\text{aromatic}}$). ^1H NMR (400 MHz, $\text{DMSO}-d_6$, δ , ppm): 7.79 (s, 1H, H-2), 8.13 (d, 1H, H-4), 7.94-7.97 (m, 2H, H-5 and H-6), 8.28 (d, 1H, H-7), 10.17 (s, 1H, -NH, D_2O -exchangeable), 8.09 (s, 1H, $=\text{CH}_{\text{olifinic}}$), 7.39 (d, 1H, H-3'), 7.13-7.15 (m, 1H, H-4'), 7.58 (d, 1H, H-5'). ^{13}C NMR (100 MHz, $\text{DMSO}-d_6$, δ , ppm): 127.50 (C-2), 110.16 (C-3), 118.09 (C-4), 119.36 (C-5), 122.92 (C-6), 111.32 (C-7), 128.19 (C-3a), 137.43 (C-7a), 136.84 (C-2'), 126.27 (C-3'), 129.05 (C-4'), 131.56 (C-5'), 114.49 (C-1'), 153.90 (C-2'), 118.09 (CN). MS (EI): (m/z) 250.06 [M^+].

4.4.14 (E)-3-(5-Methyl-1H-indol-3-yl)-2-(thiophen-2-yl)acrylonitrile (3n)

Yellow solid, yield 94 %, m.p. 196 °C, Analytical cal. $\text{C}_{16}\text{H}_{12}\text{N}_2\text{S}$: C, 72.70; H, 4.58; N, 10.60; found: C, 72.70; H, 4.55; N, 10.63. IR (KBr cm^{-1}): 2217 ($\text{C}\equiv\text{N}$), 1560, 1445 ($\text{C}=\text{C}_{\text{aromatic}}$). ^1H NMR (400 MHz, $\text{DMSO}-d_6$, δ , ppm): 7.79 (s, 1H, H-2), 7.42 (s, 1H, H-4), 7.08 (d, 1H, H-6), 7.09 (d, 1H, H-7), 2.56 (s, 3H, $-\text{CH}_3$), 10.02 (s, 1H, -NH, D_2O -exchangeable), 7.99 (s, 1H, $=\text{CH}_{\text{olifinic}}$), 7.37 (d, 1H, H-3'), 7.15 (m, 1H, H-4'), 7.68 (d, 1H, H-5'). ^{13}C NMR (100 MHz, $\text{DMSO}-d_6$, δ , ppm): 127.81 (C-2), 110.42 (C-3), 120.58 (C-4), 129.34 (C-5), 121.82 (C-6), 111.90 (C-7), 126.62 (C-3a), 134.22 (C-7a), 136.74 (C-2'), 126.91 (C-3'), 127.90 (C-4'), 131.16 (C-5'), 114.81 (C-1'), 153.32 (C-2'), 118.16 (CN), 21.30 (CH_3). MS (EI): (m/z) 264.07 [M^+].

4.4.15 (E)-3-(5-Hydroxy-1H-indol-3-yl)-2-(thiophen-2-yl)acrylonitrile (3o)

Light yellow solid, yield 95 %, m.p. 202 °C, Analytical cal. $\text{C}_{15}\text{H}_{10}\text{N}_2\text{OS}$: C, 67.65; H, 3.78; N, 10.52; found: C, 67.66; H, 3.75; N, 10.54. IR (KBr cm^{-1}): 2219 ($\text{C}\equiv\text{N}$), 1562, 1448 ($\text{C}=\text{C}_{\text{aromatic}}$). ^1H NMR (400 MHz, $\text{DMSO}-d_6$, δ , ppm): 7.78 (s, 1H, H-2), 7.40 (s, 1H, H-4), 7.18 (d, 1H, H-6), 7.29 (d, 1H, H-7), 5.35 (s, 1H, $-\text{OH}$, D_2O -exchangeable), 10.06 (s, 1H, -NH, D_2O -exchangeable), 8.07 (s, 1H, $=\text{CH}_{\text{olifinic}}$), 7.32 (d, 1H, H-3'), 7.18 (m, 1H, H-4'), 7.60 (d, 1H, H-5'). ^{13}C NMR (100 MHz, $\text{DMSO}-d_6$, δ , ppm): 127.20 (C-2), 110.42 (C-3), 120.50 (C-4), 129.32 (C-5), 121.84 (C-6), 112.56 (C-7), 125.62 (C-3a), 134.07 (C-7a), 135.71 (C-2'), 126.90 (C-3'), 127.91 (C-4'), 131.15 (C-5'), 114.83 (C-1'), 152.32 (C-2'), 118.71 (CN). MS (EI): (m/z) 277.06 [M^+].

4.5 Density Functional Theory (DFT) Calculations

The density functional theory (DFT) calculations were conducted with a hybrid functional B3LYP (Becke's three parameters nonlocal exchange function with the Lee-

Yang-Parr correlation function) [62, 63] at the 6-311G basis set using the GAMESS interface in ChemBio3D ultra ver. 14.0 (PerkinElmer, MA, USA).

Acknowledgments Shaista Azaz, thanks the Chairman, Department of Chemistry, AMU, Aligarh, for providing the necessary research facilities, University Sophisticated Instrumentation Facility (USIF), AMU, Aligarh and Sophisticated Analytical Instrumentation Facility (SAIF), Chandigarh, is credited for spectral analysis. UGC is also gratefully acknowledged for research fellowship to S. Azaz and F. Ahmad.

References

1. Trost BM (1991) *Science* 254:1471
2. Parveen M, Azaz S, Malla AM, Ahmad F, Silva PSPD, Silva MR (2015) *New J Chem* 39:469
3. Shylesh S, Schünemann V, Thiel WR (2010) *Angew Chem Int Ed* 49:3428
4. Parveen M, Azaz S, Malla AM, Ahmad F, Ahmad M, Gupta M (2016) *RSC Adv* 6:148
5. Clark JH (2002) *Acc Chem Res* 35:791
6. Princy G, Satya P (2014) *Catal Today* 236:153
7. Parveen M, Ahmad F, Malla AM, Alam M, Lee DU (2014) *Catal Lett* 144:2091
8. Parveen M, Ahmad F, Malla AM, Azaz S (2015) *New J Chem* 39:2028
9. Wang L, Zhao W, Tan W (2008) *Nano Res* 1:99
10. Gupta P, Paul S (2011) *Green Chem* 13:2365
11. Gupta P, Paul S (2014) *Curr Catal* 3:53
12. Gupta P, Paul S (2012) *J Mol Catal A Chem* 352:75
13. Gupta P, Kour M, Paul S, Clark JH (2014) *RSC Adv* 4:7461
14. Gupta P, Kumar V, Paul S (2010) *J Braz Chem Soc* 21:349
15. Zolfigol MA, Ayazi-Nasrabadi R, Bagheri S (2016) *Appl Organomet Chem* 30:273
16. Knoevenagel E (1898) *Ber Dtsch Chem Ges* 31:2585
17. Bigi F, Chesini L, Maggi RR, Sartori G (1999) *J Org Chem* 64:1033
18. Yu N, Aramini JM, Germann MW, Huang Z (2000) *Tetrahedron Lett* 41:6993
19. Parveen M, Malla AM, Alam M, Ahmad M, Rafiq S (2014) *New J Chem* 38:1655
20. Gawande MB, Jayaram RV (2006) *Catal Commun* 7:931
21. Mukarram SMJ, Khan RAR, Yadav RP (2007) *US Pat* 0004935
22. Madivada LR, Anumala RR, Gilla G, Alla S, Charagondla K, Kagga M, Bhattacharya A, Bandichhor R (2009) *Org Process Res Dev* 13:1190
23. Beutler U, Fuenfschilling PC, Steinkemper A (2007) *Org Process Res Dev* 11:470
24. Tietze LF, Beifuss U (1991) In: Trost BM, Fleming I (eds) *Comprehensive organic synthesis*, vol 2. Pergamon Press, Oxford, p 341
25. Carta A, Palomba M, Boatto G, Busonera B, Murreddu M, Loddo R (2004) *II Farmaco* 59:637
26. Quiroga J, Cobo D, Insuasty B, Abonia R, Noguera M, Cobo J, Vasquez Y, Gupta M, Derita M, Zacchino S (2007) *Arch Pharm* 340:603
27. Hranjec M, Pavlovic G, Marjanovic M, Kralj M, Zamola GK (2010) *Eur J Med Chem* 45:2405
28. Saczewski F, Stencel A, Bienczak AM, Langowska KA, Michaelis M, Werel W, Halasa R, Reszka P, Bednarski P (2008) *Eur J Med Chem* 43:1847

29. Sanna P, Carta A, Nikookar MER (2000) *Eur J Med Chem* 35:535
30. Biradar JS, Sasidhar BS (2011) *Eur J Med Chem* 46:6112
31. Litina EPDH, Litinas K, Geromichalos G (2014) *Molecules* 19:9655
32. Sanna P, Carta A, Gherardini L, Nikookar MER (2002) *Farmaco* II 57:79
33. Glazer EA, Chappel LR (1982) *J Med Chem* 25:766
34. Ali A, Bliese M, Rasmussen JM, Sargent RM, Saubern S, Sawutz DG, Wilkie JS, Winkler DA, Winzenberg KN, Woodgate RCJ (2007) *Bioorg Med Chem Lett* 17:993
35. Lieber S, Scheer F, Meissner W, Naruhn S, Adhikary T, Brüsselbach SM, Diederich WE, Muller R (2012) *J Med Chem* 55:2858
36. Janssen PAJ, Lewi PJ, Arnold E, Daeyaert F, Jonge M, Heeres J, Luc Koymans MH, Vinkers HM, Guillemont J, Pasquier E, Kukla M, Ludovici D, Andries K, Bethune M, Pauwels R, Das K, Clark AD Jr, Frenkel YV, Hughes SH, Medaer IB, Knaep FD, Bohets H, Clerck FD, Lampo A, Williams P, Stoffels P (1901) *J Med Chem* 48:1901
37. Wolfgang K, Ulrich S (2007) *Modern crop protection compounds*, vol 445. Wiley, New York
38. Chircop M, Perera S, Mariana A, Lau H, Ma MPC, Gilbert J, Jones NC, Gordon CP, Young KA, Morokoff A, Sakoff J, O'Brien TJ, McCluskey A, Robinson PJ (2011) *Mol Cancer Ther* 10:1553
39. Yi LW, Hai XQ, Xiang MY, Min LY, Li DN, Peng GD (2001) *J Org Chem* 625:128
40. El-Tammany S, Raulfs FW, Hopf H (1983) *Angew Chem Int Ed Engl* 22:633
41. Masllorens J, Manas MM, Quintana AP, Pleixats R, Roglans A (2002) *Synthesis* 13:1903
42. Thirupathi G, Venkatanarayana M, Dubey PK, Kumari YB (2012) *Der Pharm Chem* 4:1897
43. Tarleton M, Gilbert J, Sakoff JA, McCluskey A (2012) *Eur J Med Chem* 57:65
44. Biradar JS, Sasidhar BS (2011) *Eur J Med Chem* 46:6112
45. Karmakar B, Nayak A, Banerji J (2012) *Tetrahedron Lett* 53:5004
46. Abaee MS, Mojtahedi MM, Zahedi MM, Khanalizadeh G (2006) *ARKIVOC* 15:48
47. Yadav JS, Rao PP, Sreenu D, Rao RS, Kumar VN, Nagaiah K, Prasad AR (2005) *Tetrahedron Lett* 4:7249
48. Boulet FT, Foucaud A (1982) *Tetrahedron Lett* 23:4927
49. Morrison DW, Forbes DC, Davis JH (2001) *Tetrahedron Lett* 42:6053
50. Harjani JR, Nara SJ, Salunkhe MM (2002) *Tetrahedron Lett* 43:1127
51. Tahmassebi D, Wilson LJA, Kieser JM (2009) *Synth Commun* 39:2605
52. Mulla SAR, Sudalai A, Pathan MY, Siddique SA, Inamdar SM, Chavan SS, Reddy RS (2012) *RSC Adv* 2:3525
53. Nemati F, Heravi MM, Rad RS (2012) *Chin J Catal* 33:1825
54. Mukhopadhyay C, Ray S (2011) *Catal Commun* 12:1496
55. Malla AM, Parveen M, Ahmad F, Azaz S, Alam M (2015) *RSC Adv* 5:19552
56. Parveen M, Ahmad F, Malla AM, Azaz S, Silva MR, Silva PSP (2015) *RSC Adv* 5:52330
57. Vafaezadeh M, Hashemi MM, Fard MS (2012) *Catal Commun* 26:54
58. Ilczyszyn MM, Ilczyszyn M (2003) *J Raman Spectrosc* 34:693
59. Elsabayy KM (2014) *Int J Pharm Res Health Sci* 2:70
60. Maleki A, Alrezvani Z, Maleki S (2015) *Catal Commun* 69:29
61. Niknam K, Saberi D (2009) *Tetrahedron Lett* 50:5210
62. Becke AD (1993) *J Chem Phys* 98:5648
63. Lee C, Yang W, Parr RG (1988) *Phys Rev B* 37:785